Eur. Phys. J. C 5, 723–737 (1998)
DOI 10.1007/s100529800878

THE EUROPEAN PHYSICAL JOURNAL C

Neutralino Cascades in the (M+1)SSM

U. Ellwanger, C. Hugonie

Laboratoire de Physique Théorique et Hautes Energies, Université de Paris-Sud, F-91400 Orsay, France

Received: 10 December 1997 / Revised version: 26 January 1998 / Published online: 26 March 1998

Abstract. In the (M+1)SSM an additional gauge singlet Weyl spinor appears in the neutralino sector. For a large part of the parameter space this approximative eigenstate is the true LSP. Then most sparticle decays proceed via an additional cascade involving the NLSP $\rightarrow$ LSP transition, where the NLSP is the non-singlet next-to-lightest neutralino. We present a comprehensive list of all processes, which contribute to the NLSP $\rightarrow$ LSP transition, the partial widths and the total NLSP decay rate. We perform a scan of the parameters of the model compatible with universal soft terms, and find that the NLSP life time can be quite large, leading to macroscopically displaced vertices. Our results imply that the signatures for sparticle production in the (M+1)SSM can be very different from the MSSM, and are important for calculations of the abundance of dark matter in this model.

1 Introduction

The supersymmetric extension of the standard model with an additional singlet superfield [1–8] has some attractive features: the superpotential can be chosen to be scale invariant, hence the only dimensionful parameters – and thus the electroweak scale – enter via the soft supersymmetry breaking terms. With a scale-invariant superpotential, and assuming universal soft terms at the GUT scale, the model has the same number of free parameters as the MSSM. Several analyses of the parameter space of the model have previously been performed in [4,5]. It has been found that a considerable region is consistent both with theoretical constraints (correct $SU(2)_L \times U(1)_Y$ symmetry breaking, no squark or slepton vev's, neutral LSP) and experimental lower bounds on sparticle and Higgs masses.

It is very important to investigate in what respect the phenomenology of the (M+1)SSM differs from that of the MSSM. The signatures for sparticle production could be different, and one would like to know which processes could serve to distinguish the two models.

The particle content of the (M+1)SSM differs from the MSSM in the form of additional gauge singlet states in the Higgs sector (1 neutral CP-even and 1 CP-odd state) and in the neutralino sector (a two component Weyl fermion). These states are mixed with the corresponding ones of the MSSM, and the physical states have to be obtained from the diagonalization of the mass matrices in the corresponding sectors. An interesting result of the analyses in [4,5] is that, for most of the parameter space, the mixing angles involving the singlet states are actually quite small. Consequently there exist physical *quasi singlet* states which have only small couplings to the gauge bosons and the MSSM sparticles such as charginos, squarks and sleptons. These states then have only small production cross sections and it seems to be nearly impossible to observe them in present or future experiments.

A notable exception can occur, however, in the neutralino sector. In the MSSM the neutralino sector consists of two gauginos (the bino and the neutral wino) and two higgsinos. Typically the LSP – the lightest supersymmetric particle, which is stable if one assumes, as we do, R-parity conservation – is the lightest eigenstate of the neutralino mass matrix. The LSP will appear as one of the final states of each sparticle decay, and its non-observability is responsible for the well-known missing energy/momentum signature of sparticle production.

The situation in the (M+1)SSM, where a singlino state is added to the neutralino sector, depends crucially on its mass with respect to the MSSM LSP mass: If the singlino is heavier, it will very rarely be produced and it will be practically unobservable. If it is lighter (and is thus the true LSP), it will now appear at the end of the decay chain of sparticles decays. To be more specific, from the analyses performed in [5] one finds that the MSSM LSP, within the allowed parameter space of the (M+1)SSM, is essentially a bino. In the singlino LSP case of the (M+1)SSM one has to keep in mind the small couplings of the singlino to all the other particles. If the sparticles are heavier than the bino (which turns out to be always the case, except for some large supersymmetry breaking terms that yield sparticles out of reach for LEP2) they thus prefer to decay into the bino to which they couple more strongly. Only then the bino will decay into the singlino LSP, which will give rise to an additional cascade in the sparticle decay chain. Since this process modifies the signatures for sparticle production considerably, we will investigate the bino to singlino transition in detail in this paper.

Production and decay of neutralinos have previously been discussed in the MSSM in, e.g., [9] and in the

(M+1)SSM in [7]. (Many of the formulas of the partial decay widths in our appendix D can be found in these papers.) In [7] production cross sections and branching ratios of neutralinos in the (M+1)SSM have been presented for several scenarios concerning the low energy parameters.

Here, however, we are interested in a comprehensive analysis of the part of the parameter space of the (M+1)SSM which is compatible with universal soft terms at the GUT scale, which corresponds to the case of a singlino LSP, and where sparticle production is kinematically possible at LEP2. Our aim is to see, which bino lifetimes and bino branching ratios are possible under these assumptions. With our results at hand one can decide, which signatures for sparticle production (beyond the ones of the MSSM) are most promising in the framework of the (M+1)SSM, and which part of the parameter space can be tested.

Our approach follows closely the one of [5], up to slightly different experimental constraints on the parameter space: We start to scan the complete parameter space of the model (the universal soft terms and Yukawa couplings, see the next section) as defined at the GUT scale. For each point in the parameter space we compute the effective parameters at low energy by integrating the renormalization group equations from M_{GUT} down to M_Z. Then, for each set of parameters, we minimize numerically the effective potential including the one loop radiative corrections induced by top quark and squark loops. We check whether the absolute minimum of the potential breaks $SU(2)_L \times U(1)_Y$ as desired, whether squarks or sleptons do not assume vev's, and whether the physical masses of the top quark and the sparticles satisfy the (model independent) present experimental constraints. (Details are given in the next section.) Finally we require that the LSP, $\tilde{\chi}_1^0$, is essentially a singlino state (otherwise the signatures for sparticle production are not different from the MSSM), and that the mass of the NLSP $\tilde{\chi}_2^0$ (which is the bino) is below M_Z. Under this approximate condition sparticle production at LEP2 is kinematically allowed.

For each of the $\sim 10^4$ remaining points in the parameter space, we compute the following decay widths: $\tilde{\chi}_2^0 \to \tilde{\chi}_1^0 l^+ l^-$, $\tilde{\chi}_2^0 \to \tilde{\chi}_1^0 \nu \bar{\nu}$, $\tilde{\chi}_2^0 \to \tilde{\chi}_1^0 q \bar{q}$ (in all cases we take Z, Higgs and slepton or squark exchange into account), $\tilde{\chi}_2^0 \to \tilde{\chi}_1^0$+Higgs and $\tilde{\chi}_2^0 \to \tilde{\chi}_1^0 + \gamma$. (The radiative decays into a photon have previously been considered in the MSSM in, e.g., [10,11], and in the (M+1)SSM in [7].) The results give us both the life time and the branching ratios of the NLSP $\to$ LSP transition for each point in the parameter space of the model, which is consistent with universal soft terms, present experimental constraints, and which is of potential phenomenological relevance for LEP2.

Clearly many steps of this procedure (e.g. the integration of the RGEs, the minimization of the effective potential, the diagonalization of the mass matrices and the phase space integrals) require numerical methods. These allow us, however, to obtain the results with satisfactory accuracy. On the other hand, we find it very desirable to understand at least the rough features of our results (and of the range of the low energy parameters) using analytic approximations to the integrated RGEs, the minimization of the effective potential, and the diagonalization of the mass matrices. Therefore we spend some time in Sect. 3 in order to discuss the interplay between the different theoretical and experimental constraints on the parameters within such analytic approximations. These approximations allow us to understand the relative importance and the orders of magnitude of the different decay widths in Sect. 4. The results on the different decay widths, branching ratios and the total life time presented in Sect. 4 (and in the figures) are, however, based on the "exact" numerical procedure.

Our results show that, even in the limit of tiny couplings of the singlino, a priori a large number of different processes can contribute to the bino to singlino transition. Only after a detailed investigation of all the partial widths we find that only a few of them are relevant: Essentially the three body decays with two leptons in the final state (via virtual slepton exchange) or with $q\bar{q}$ in the final state (via virtual Z exchange), and in some cases the two body decay into a real singlet Higgs scalar or a photon. Interestingly enough we find that, for small enough Yukawa couplings, the lifetime of the bino becomes so large that displaced vertices appear to be visible.

Two cosmological issues should also be discussed within the (M+1)SSM, namely domain walls and dark matter. The (M+1)SSM with a scale invariant superpotential has a discrete $\mathbb{Z}_3$ symmetry, which can lead to the formation of domain walls with an unacceptable energy density during the electroweak phase transition [6]. As discussed in [6], possible ways out of this problem are to embed the discrete symmetry into a gauge symmetry at some large scale, or to add tiny mass terms, which do not modify the phenomenology in a visible way, but which break the $\mathbb{Z}_3$ symmetry sufficiently such that the domain walls are removed.

The LSP of any supersymmetric theory with conserved R parity is a priori a welcome candidate for cold dark matter. It will necessarily be produced in sparticle decays in the early universe, and its relic density will strongly depend on its annihilation cross section. The (M+1)SSM has been considered in this respect in [8], where both upper and lower limits on the LSP relic density have been imposed. In [8] it has been argued that the singlino LSP scenario of the (M+1)SSM is essentially ruled out, since the pair annihilation cross section is too small, and consequently the relic density is too large. However, in [8] only the LSP pair annihilation has been considered. In particular in the case of small Yukawa couplings the situation for a singlino LSP is, however, much more complicated: The binos could pair annihilate before the LSP is produced, and the bino-singlino coannihilation rate is much larger than the singlino pair annihilation rate. In order to determine the dark matter constraints in the (M+1)SSM with singlino LSP reliably it is thus absolutely necessary to know the bino lifetime or the bino to singlino decay rate. Apart from the modified signatures for sparticle production the results of this paper will thus also find ap-

plications in the investigation of the dark matter in the (M+1)SSM.

The paper is organized as follows: In the next section we present the lagrangian and discuss briefly the method of the scanning of the acceptable parameter space; this procedure follows the one of [5]. In section three we study the range of parameters in the singlino LSP scenario in some detail, focussing on analytic approximations. In section four we investigate all possible bino to singlino decay channels, the corresponding contributions to the partial bino decay widths, and the bino lifetime. We present both approximate analytic results, and "exact" results based on the numerical procedure. In section five we discuss our results and its phenomenological consequences.

2 Parameter Space of the (M+1)SSM

In this section, we study the parameter space of the model with the same assumptions as in [5]. The superpotential of the (M+1)SSM is given by

$$W = \lambda H_1 H_2 S + \frac{1}{3}\kappa S^3 + \dots \tag{1}$$

where the ellipsis stand for quarks and leptons Yukawa couplings,

$$H_1 = \begin{pmatrix} H_1^+ \\ H_1^0 \end{pmatrix}, \quad H_2 = \begin{pmatrix} H_2^0 \\ H_2^- \end{pmatrix}$$
$$\text{and} \quad H_1 H_2 = H_1^+ H_2^- - H_1^0 H_2^0. \tag{2}$$

Here the Higgs doublet H_1 couples to the up-type quarks, and H_2 to the down-type quarks and the charged leptons. Therefore the usual parameter β is given by

$$\tan\beta = \frac{h_1}{h_2} \tag{3}$$

with $h_i = \langle H_i^0 \rangle$. S denotes the gauge singlet superfield beyond the MSSM. The superpotential contains no $\mu H_1 H_2$ term. An effective μ term is generated once the scalar component of the singlet S acquires a vev s:

$$\mu = \lambda s. \tag{4}$$

The only dimensionful parameters of the model are the supersymmetry breaking gaugino masses, scalar masses and trilinear couplings (for simplicity we do not display the terms involving squarks or sleptons):

$$\begin{aligned} \mathcal{L}_{soft} = & \frac{1}{2}\left(M_3 \lambda_3^a \lambda_3^a + M_2 \lambda_2^i \lambda_2^i + M_1 \lambda_1 \lambda_1\right) + \text{ h.c.} \\ & - m_1^2 |H_1|^2 - m_2^2 |H_2|^2 - m_S^2 |S|^2 \\ & - \lambda A_\lambda H_1 H_2 S - \frac{1}{3}\kappa A_\kappa S^3 + \text{ h.c.} \end{aligned} \tag{5}$$

λ_1, λ_2 and λ_3 are the gauginos of the $U(1)_Y$, $SU(2)_L$ and $SU(3)_c$ gauge groups respectively. The scalar components of the Higgs in (5) are denoted by the same letters as the corresponding chiral superfields.

The scalar potential contains the standard F and D terms, the supersymmetry breaking terms and one loop radiative corrections of the form

$$V_{rad} = \frac{1}{64\pi^2} \mathrm{STr}\mathcal{M}^4 \ln\left(\frac{\mathcal{M}^2}{Q^2}\right). \tag{6}$$

In (6) we take into account only top quark and squark loops, but we include the numerically important contributions beyond the leading log approximation which result from the complete top squark mass matrix. Q^2 denotes the renormalization point, and all the parameters in (1), (5) and (6) have to be taken at the scale $Q^2 \sim M_Z^2$.

The supersymmetry breaking terms of the model are constrained by requiring universal terms at the scale $M_{GUT} \sim 10^{16}$ GeV. The independent parameters of the model are thus universal gaugino masses M_0 (always positive in our convention), a universal mass for the scalars m_0^2, a universal trilinear coupling A_0 (either positive or negative), and the Yukawa couplings λ_0 and κ_0 of the superpotential (1) at the scale M_{GUT}. In addition the top quark Yukawa coupling affects the renormalization group evolution of the parameters from M_{GUT} down to the electroweak scale. The value of the Z mass fixes one of these parameters with respect to the others, so that we end up with 5 free parameters at the GUT scale, as many as in the MSSM with universal soft terms.

Following the same procedure as in [5], we perform a scan over the complete parameter space of the model at M_{GUT}, integrate the renormalization group equations (RGE) down to the electroweak scale, and minimize the low energy effective potential including the radiative corrections (6) numerically in each case. We check whether we have found the absolute minimum of the potential, and verify whether squarks or sleptons do not assume vev's, which would break color and/or electromagnetism. Already at this stage, the condition to avoid selectron vev's (which are the most dangerous ones) yields a constraint on the parameter space [5]:

$$\frac{A_0}{M_0} \gtrsim -2.5 \tag{7}$$

In the remaining cases we diagonalize numerically the mass matrices, compute the physical masses of all particles and impose the following experimental constraints:

$$\begin{aligned} & m_{\tilde{\nu}} > M_Z/2 \text{ GeV} \quad [12], \\ & m_t = 175 \pm 6 \text{ GeV} \quad [13]. \end{aligned} \tag{8}$$

Note that, since signatures for sparticles production in the present scenario may be different from the MSSM, we cannot apply the standard MSSM analysis to the latest data from LEP1.5 and LEP2. This data should rather be reanalysed, in the context of the (M+1)SSM, using the results of the present paper. However, the LEP1 results on the Z width and thus the sneutrino mass $m_{\tilde{\nu}}$ remain valid. Moreover it turns out that the essential properties of the neutralino sector do not depend on the details of the lower limits on, e.g., the chargino or slepton masses.

Furthermore, within the present assumption of universality of the soft parameters at the GUT scale and the singlino LSP scenario, (8) imply already strong constraints on the other new particle masses (cf Sect. 3), so that nearly all the other experimental bounds turn out to be automatically satisfied:

$$\begin{aligned} & m_{\chi_i^0} + m_{\chi_j^0} > M_Z \\ & \quad or\ \Gamma(Z \to \tilde{\chi}_i^0 \tilde{\chi}_j^0) < \ 7\,\mathrm{MeV} \quad \text{if} \quad (i,j) = (1,1), \\ & \qquad \Gamma(Z \to \tilde{\chi}_i^0 \tilde{\chi}_j^0) < 30\,\mathrm{MeV} \quad \text{if} \quad (i,j) \neq (1,1), \\ & m_{H^\pm} > 150\,\mathrm{GeV}, \, m_{A^0} > 130\,\mathrm{GeV}, \\ & m_{\tilde{t}_1} > 190\,\mathrm{GeV}, \quad m_{\tilde{g}} > 280\,\mathrm{GeV}, \\ & m_{\chi_1^\pm} > 60\,\mathrm{GeV}, \quad m_{\tilde{l}_R} > 60\,\mathrm{GeV} \end{aligned}$$

where A^0 is the lightest non-singlet neutral CP-odd Higgs. The lightest non-singlet CP-even Higgs is in the range from 100 GeV up to 140 GeV.

As emphasized in [4,5], the allowed parameter space of the (M+1)SSM is in general characterized by small values of the Yukawa couplings λ and κ ($\lambda, \kappa \lesssim 0.3$). As we will see in the next section the singlino LSP case corresponds to even smaller values of the Yukawa couplings $\lambda, \kappa \lesssim 10^{-2}$.

3 Singlino LSP scenario

In this section we present some special features of the singlino LSP scenario. In particular, we derive some approximative constraints on the high energy free parameters and some analytic approximations for the low energy masses and mixing factors. These approximations are useful to understand the features of our numerical results and will provide us with helpful guidelines for the calculations of the next section. To this end we use approximate relations between the low energy and high energy parameters of the model (as obtained from the RGEs), and relations obtained from the minimization of the tree level potential. At the beginning we assume that the Yukawa couplings λ and κ are small, but this assumption will be justified below.

In order to derive the constraints on the parameters implied by the singlino LSP scenario we first have to find approximate expressions for the singlino and the lightest non-singlet neutralino masses.

Let us start with the singlino mass M. From the neutralino mass matrix (61) of Appendix A one finds that the mixing of the singlino to the higgsinos is proportional to λ and thus relatively small. Hence, the singlino remains an almost pure state, and its mass is

$$M = 2\kappa s. \tag{9}$$

Using the minimization of the tree level potential the vev s and hence M can be related to the bare parameters of the model: For small Yukawa couplings (and hence $s \gg h_1, h_2$) the minimization equation (69) for the singlet becomes

$$s \simeq -\frac{A_\kappa}{4\kappa}\left(1 + \sqrt{1 - \frac{8 m_S^2}{A_\kappa^2}}\right). \tag{10}$$

A_κ and m_S being only slightly renormalized between M_{GUT} and M_Z (cf Appendix C), one obtains the singlino mass in terms of the GUT parameters:

$$M \simeq -\frac{A_0}{2}\left(1 + \sqrt{1 - \frac{8 m_0^2}{A_0^2}}\right). \tag{11}$$

Note that M has the sign opposite to A_0. The condition for the minimum (10) to be deeper than the symmetric one ($h_1 = h_2 = s = 0$) reads

$$A_0^2 \gtrsim 9 m_0^2, \tag{12}$$

so that

$$\frac{2}{3}|A_0| \lesssim |M| \lesssim |A_0|. \tag{13}$$

Next, we estimate the masses of the lightest non-singlet neutralinos. The higgsino effective mass term $\mu = \lambda s$ turns out to be quite large (see below). Since the mixing terms between the gauginos and the higgsinos are at most of $O(M_Z/2\mu)$, one finds that, to a good approximation, the lightest non-singlet neutralinos are the (nearly pure) bino and the wino. Their masses M_1 and M_2 are related to M_0 as given in appendix C:

$$M_1 \simeq .5 M_2 \simeq .41 M_0. \tag{14}$$

The condition for the singlino to be the LSP is given by $M < M_1$, which, combined with (13) and (14), yields

$$|A_0| \lesssim .6 M_0. \tag{15}$$

(Note that this condition is compatible with the necessary condition for the absence of color and/or electromagnetism breaking vevs, (7).) Equation (15) together with (12) implies that the singlino LSP scenario discards large $|A_0|/M_0$ and m_0^2/M_0^2 ratios, and it just corresponds to a very natural "gaugino dominated scenario", gaugino masses being the largest soft terms. Then, the masses of all non-singlet sparticles can be expressed in terms of M_0 and are therefore strongly correlated.

For later use it is convenient to introduce a parameter η, defined by the ratio of the masses of the lightest and next-to-lightest neutralinos:

$$\eta = \frac{m_{\chi_1^0}}{m_{\chi_2^0}} \simeq \frac{M}{M_1}. \tag{16}$$

Unlike in the MSSM, it is not fixed by universality constraints at the GUT scale, but it is rather a free parameter varying from -1 to $+1$. Equations (13) and (14) allow us to express η easily in terms of the bare parameters A_0 and M_0:

$$\eta \sim -2\frac{A_0}{M_0}. \tag{17}$$

Next, we wish to estimate the higgsino effective mass term $\mu = \lambda s$, and show that it is quite large. Below, the

knowledge of μ will allow us to relate η to the Yukawa coupling λ. First, the minimization of the tree level potential with respect to h_1 and h_2 gives the relation

$$\tan^2\beta = \frac{m_2^2+\mu^2+M_Z^2/2}{m_1^2+\mu^2+M_Z^2/2}. \tag{18}$$

The condition for a non-trivial minimum corresponds to the condition that the denominator of (18) has to be positive. The approximative solutions of the RGEs (84) and (85) imply that $m_2^2>0$, whereas $m_1^2<0$. Hence one obtains

$$\mu^2 \gtrsim -m_1^2-.5M_Z^2 \gtrsim 2.1M_0^2-.5M_Z^2. \tag{19}$$

Since, in addition, phenomenological constraints imply that M_0 is quite large ($M_0 \gtrsim$ 110 GeV, see below), one finds $\mu^2 \gg M_Z^2$. Actually, from our numerical results (within the singlino LSP scenario) we find $\tan\beta \gtrsim 6$ which implies

$$\mu^2 \simeq 2.5M_0^2-.5M_Z^2. \tag{20}$$

in agreement with (19).

Next, we derive an upper limit on the Yukawa couplings within the singlino LSP scenario. First, from the absence of a deeper unphysical minimum of the Higgs potential with $h_2=s=0$, the following inequality can be derived [5]:

$$\kappa < 3.10^{-2}\frac{A_0^2}{M_0^2}. \tag{21}$$

Furthermore, from the numerical analysis, the Yukawa couplings λ and κ turn out to be closely related:

$$\kappa \sim \lambda^{1.5\pm.3}. \tag{22}$$

Using (17) in (21) and (22) one finds that the singlino LSP scenario requires small Yukawa couplings, $\lambda,\kappa \lesssim 10^{-2}$.

On the other hand, no lower limit on the Yukawa couplings has been found in our analysis; we allowed for couplings as small as $\lambda=10^{-6}$. In this regime one can show that the singlino LSP scenario follows automatically: Using (9), (4), (22) and (20), one gets

$$|M| = 2\kappa|s| = 2\kappa|\mu|/\lambda \sim 2\lambda^{.5\pm.3}|\mu| \sim 3.2\lambda^{.5\pm.3}M_0, \tag{23}$$

so that

$$|\eta| \sim 7.7\lambda^{.5\pm.3}. \tag{24}$$

Hence, for very small values of λ ($\lambda \lesssim 10^{-5}$ in our numerical analysis), the singlino LSP scenario is always realized and $\eta \ll 1$. The compatibility of (24) with (17) requires some relation between the bare parameters A_0, M_0 and λ_0 of the model which is, however, not very stringent.

Herewith we conclude the discussion of the constraints on the parameters of the model implied by the singlino LSP scenario. With the help of these results we can now obtain approximate expressions for all quantities which are required in order to calculate the bino to singlino decay widths: the mixing parameters of the singlino with the other non-singlet neutralinos, and the masses of the sfermions and the Higgs bosons. Let us first study the mixing parameters:

For $|\eta|$ not too close to 1, one can expand the singlino and the bino eigenstates in small mixing parameters in the basis of (59):

$$\begin{aligned} N_{1i} \sim \Bigg(& \frac{\lambda g_2(h_2^2-h_1^2)\mu}{\sqrt{2}(M-M_2)(M^2-\mu^2)}, \\ & \frac{\lambda g_1(h_1^2-h_2^2)\mu}{\sqrt{2}(M-M_1)(M^2-\mu^2)}, \\ & \frac{\lambda(\mu h_1 - M h_2)}{M^2-\mu^2}, \frac{\lambda(\mu h_2 - M h_1)}{M^2-\mu^2}, 1\Bigg), \end{aligned} \tag{25}$$

$$\begin{aligned} N_{2i} \sim \Bigg(& \frac{-g_1 g_2(M_1(h_1^2+h_2^2)+2\mu h_1 h_2)}{2(M_2-M_1)(M_1^2-\mu^2)}, 1, \\ & \frac{g_1(\mu h_2 + M_1 h_1)}{\sqrt{2}(M_1^2-\mu^2)}, \frac{-g_1(M_1 h_2 + \mu h_1)}{\sqrt{2}(M_1^2-\mu^2)}, \\ & \frac{\lambda g_1(h_1^2-h_2^2)\mu}{\sqrt{2}(M_1-M)(M_1^2-\mu^2)}\Bigg). \end{aligned} \tag{26}$$

Using (14), (20), (16) and $h_1 \gg h_2$, these components can be expressed in terms of η, M_1 and M_Z. (However, (25) and (26) are not valid anymore in the degenerate case $|\eta| \to 1$.) These expressions for the mixing parameters will be used extensively for the analytic approximations in the next section.

Next, we turn to the sfermion sector. The lightest states are the sneutrinos $\tilde\nu$ and the "right handed" charged sleptons $\tilde l_R$. The approximate expressions for their masses are (cf Appendix C)

$$m_{\tilde l_R}^2 = m_E^2 - \sin^2\theta_W M_Z^2\cos 2\beta \simeq .15M_0^2+.23M_Z^2, \tag{27}$$

$$m_{\tilde\nu}^2 = \quad m_L^2 + \tfrac{1}{2}M_Z^2\cos 2\beta \quad \simeq .52M_0^2-.5M_Z^2. \tag{28}$$

The lower limit on $m_{\tilde\nu}$ (8) combined with (28) gives a lower limit on M_0 ($\gtrsim$ 110 GeV), which in turn puts a lower limit on $m_{\tilde l_R}$ ($\gtrsim$ 60 GeV). "Left handed" charged sleptons and squarks are always much heavier, hence uninteresting for the present phenomenology.

The lower limit on M_0 also yields a lower limit on the bino mass: $m_{\chi_2^0} \gtrsim$ 30 GeV. Subsequently we restrict our analysis to the regime $m_{\chi_2^0} < M_Z$, where sparticle production at LEP2 (at least the pair production of binos) is kinematically allowed. In terms of M_0 this corresponds to $M_0 \lesssim$ 230 GeV. In this region of the parameter space, the bino is the NLSP. Note that for larger values of M_0 the D-term in (27) becomes negligible and one has

$$m_{\tilde l_R}^2 \simeq .15M_0^2 < M_1^2 \simeq .17M_0^2. \tag{29}$$

Thus, for $M_0 \gtrsim$ 320 GeV, $\tilde l_R$ turns out to be the NLSP. We shall come back to the case $m_{\chi_2^0} > M_Z$ in the last section.

The large value of μ implies that the lightest chargino $\chi_1^\pm$ is mainly a wino of mass M_2, which is related to M_0 by

(14). However, for small values of M_0 the higgsino component can be quite large (up to 50%) and $m_{\chi_1^\pm}$ smaller than M_2. The lower bound on M_0 yields $m_{\chi_1^\pm} \gtrsim 60$ GeV.

Similarly, from the lower bound on M_0, we obtain the lower bound on the gluino mass given in the previous section.

Finally, we briefly focus our attention on the Higgs sector. We see from the mass matrices given in Appendix B that the mixings of the CP-even and CP-odd singlets with the non-singlet Higgs fields are proportional to λ, hence small. Here again, the singlet sector decouples and we end up with two almost pure singlet states, a scalar of mass

$$M^2_{S,33} \simeq \frac{1}{4}\sqrt{A_0^2 - 8m_0^2}\left(|A_0| + \sqrt{A_0^2 - 8m_0^2}\right), \quad (30)$$

and a pseudoscalar of mass

$$M^2_{P,22} \simeq \frac{3}{4}|A_0|\left(|A_0| + \sqrt{A_0^2 - 8m_0^2}\right) \quad (31)$$

where we have used (72), (77) and (10). The pseudoscalar is always heavier than the scalar singlet and, using arguments similar to (23), one finds that their masses are both roughly proportional to $M \sim \lambda^{.5\pm.3} M_0$ in the singlino LSP case. Therefore, the singlet states are the lightest Higgs states.

In the non-singlet sector, we have one CP-odd pseudoscalar A^0 of mass

$$M^2_{P,11} \simeq \frac{0.3 M_0^2}{\sin 2\beta} \quad (32)$$

where we have used (20) and the approximate solution of the RGE for A_λ (81) in the limit $m_0, A_0 \ll M_0$. As $\tan\beta$ is always quite large, A^0 turns out to be relatively heavy as already remarked in Sect. 2. The mixing term between the CP-even fields H_{1R} and H_{2R} is proportional to:

$$\frac{M^2_{S,12}}{M^2_{S,22} - M^2_{S,11}} \sim \cot\beta \ll 1. \quad (33)$$

H_{1R} and H_{2R} are then almost pure states of mass

$$M^2_{S,11} \simeq M_Z^2, \quad (34)$$

$$M^2_{S,22} \simeq 0.3 M_0^2 \tan\beta > M^2_{S,11}. \quad (35)$$

These approximations must be taken with care, as they do not include the numerically important radiative contributions beyond the RGE to the effective potential (6). Nevertheless, we find from the numerical analysis (with the radiative corrections to the effective potential included) the following particle assignments and mass ranges in the Higgs sector, in agreement with our rough estimates:

$$\begin{array}{lccccc}
S_1 \sim S_R & 0 & \lesssim & m_{S_1} & \lesssim & 60\,\text{GeV}, \\
S_2 \sim H_{1R} & 100 & \lesssim & m_{S_2} & \lesssim & 120\,\text{GeV}, \\
S_3 \sim H_{2R} & 130 & \lesssim & m_{S_3} & \lesssim & 360\,\text{GeV}, \\
P_1 \sim S_I & 0 & \lesssim & m_{P_1} & \lesssim & 130\,\text{GeV}, \\
P_2 \sim A^0 & 130 & \lesssim & m_{P_2} & \lesssim & 350\,\text{GeV}.
\end{array}$$

However, the upper bounds given above increase if one relaxes the condition $M_1 < M_Z$, allowing for higher values of M_0.

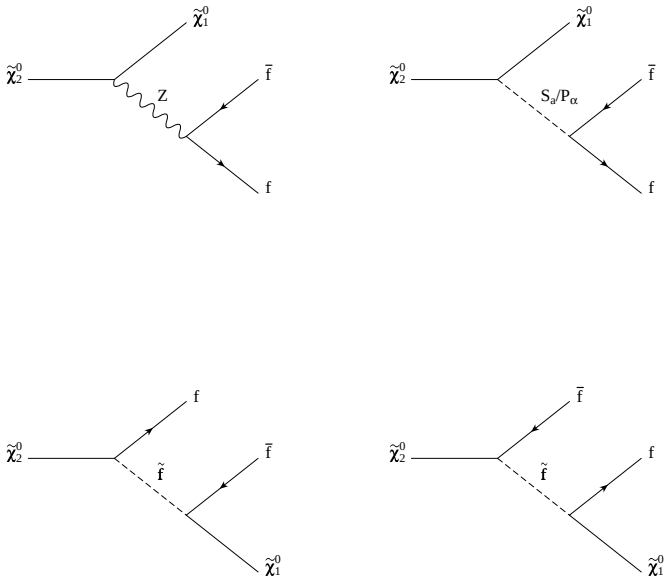

Fig. 1. Diagrams contributing to the three body decay $\tilde\chi_2^0 \to \tilde\chi_1^0 f\bar f$

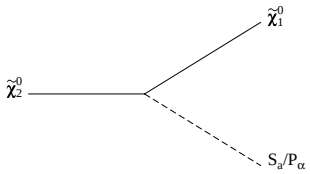

Fig. 2. Feynman graph for the two body decay $\tilde\chi_2^0 \to \tilde\chi_1^0 S_a/P_\alpha$

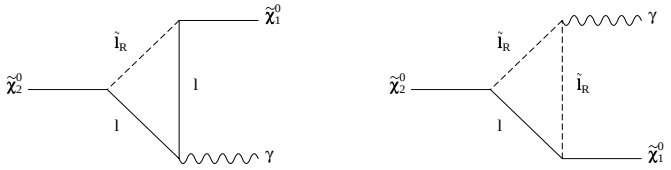

Fig. 3. Contributions to the radiative decay $\tilde\chi_2^0 \to \tilde\chi_1^0\gamma$ with only charged lepton/"right" slepton loops

4 Bino to singlino transition

In this section we compute the bino to singlino decay widths. As already mentioned, this process is crucial as it will appear at the end of every sparticle decay chain in the singlino LSP case. The different contributions are shown in Figs. 1–3. Exact formulae for the corresponding decay widths are given in Appendix D. The production and decay of neutralinos have already been studied in the (M+1)SSM framework for a few selected points in the parameter space [7]. Instead, we have computed the partial and total decay widths numerically for each point in the parameter space obtained from our numerical scanning.

In the following, we first present some simple analytic approximations so as to understand the main features of the bino to singlino transition. Then we discuss our the "exact" results, which are based on the numerical integration of the RGEs, the numerical minimization of the full

Higgs potential, the numerical computation of the mixings and mass eigenvalues in the neutralino, chargino and Higgs boson sector, and the integration of the exact phase space integrals. These results turn out to be in good agreement with the analytic approximations.

First of all, let us consider the tree level three body decay $\tilde{\chi}_2^0 \to \tilde{\chi}_1^0 f \bar{f}$ of Fig. 1. The fermions can be charged leptons, neutrinos or quarks (in which case we end up with two jets). All the decay widths are proportional to λ^2 – one factor λ from the non-singlet component of the singlino, raised to the square – and are hence equally suppressed. Therefore, for each final state, we have to check whether the virtual Z, sfermion or Higgs exchange gives the main contribution and whether we have to compute interference terms.

Let us start with a pair of charged leptons in the final state. The partial width via virtual Z exchange is given by (97) [9]. It depends on the mixing factor O_{12} in the coupling $Z\tilde{\chi}_1^0\tilde{\chi}_2^0$ defined by (95), and a phase space integral I_Z defined by (98). In our analytic approximations we assume a very light singlino, i.e. η small. (We shall come back later to the case $\eta \not\to 0$.) Using (25) and (26) in the limit of large $\tan\beta$ and $|\eta| \ll 1$, the mixing factor O_{12} can be written

$$O_{12} \simeq 1.7\,10^{-2}\lambda \left(\frac{M_Z}{M_1}\right)^2. \tag{36}$$

As we take $|\eta|$ small, the phase space integral I_Z is of $O(10^{-1})$, so that the decay width reads

$$\begin{aligned}\Gamma(\tilde{\chi}_2^0 \xrightarrow{Z} \tilde{\chi}_1^0 l^+ l^-) &\simeq 6.10^{-9}\lambda^2 M_1 I_Z(\eta,\omega_Z)\\ &\sim 10^{-10}\lambda^2 M_1.\end{aligned} \tag{37}$$

For the slepton exchange, the partial width is given by (108) [9]. Since the "left" type charged sleptons are always much heavier than the "right" type ones, their contribution will be relatively unimportant. The vertex factor involves the mixing factor N_{12} defined in (62). Using (25) with the same assumptions as above yields

$$\sqrt{2}\, g_1 N_{12} \simeq .13\lambda \left(\frac{M_Z}{M_1}\right)^2. \tag{38}$$

The partial width then reads

$$\Gamma(\tilde{\chi}_2^0 \xrightarrow{\tilde{l}_R} \tilde{\chi}_1^0 l^+ l^-) \simeq 2.10^{-6}\lambda^2 M_1 \left(\frac{M_Z}{m_{\tilde{l}_R}}\right)^4 I_{\tilde{l}_R}(\eta,\omega_{\tilde{l}_R}). \tag{39}$$

As for the Z exchange, the phase space integral $I_{\tilde{l}_R}$, given by (109), is of $O(10^{-1})$. One can infer from (27) that the ratio $M_Z/m_{\tilde{l}_R}$ is always of $O(1)$. Equation (39) then gives

$$\begin{aligned}\Gamma(\tilde{\chi}_2^0 \xrightarrow{\tilde{l}_R} \tilde{\chi}_1^0 l^+ l^-) &\sim 10^{-7}\lambda^2 M_1\\ &\gg \Gamma(\tilde{\chi}_2^0 \xrightarrow{Z} \tilde{\chi}_1^0 l^+ l^-)\end{aligned} \tag{40}$$

In the case of virtual Higgs exchange, the partial width is given by (103) and depends, in this case, on the mixing factors Q_{a12} and Q_{al} defined in (99), (101), respectively. (Here and below the index l denotes a charged lepton and replaces the index f in (101).) First, we observe that if the lightest Higgs scalar (which is the singlet) is too heavy to be produced on shell, the partial width for its virtual exchange is proportional to λ^6, and hence completely negligible:

$$\begin{aligned}&Q_{112} \sim \lambda^2 \quad \text{and} \quad Q_{1l} \sim \lambda\\ \Longrightarrow \qquad &\Gamma(\tilde{\chi}_2^0 \xrightarrow{S_R} \tilde{\chi}_1^0 l^+ l^-) \sim \lambda^6.\end{aligned} \tag{41}$$

The result is similar for the singlet pseudoscalar S_I, which is always heavier than S_R. As shown in the previous section, the second scalar S_2 is mainly H_{1R}, so that

$$Q_{212} \simeq \frac{\lambda}{\sqrt{2}} N_{24} - \frac{g_1}{2} N_{13} \simeq \frac{\lambda g_1 h_1}{\mu}, \tag{42}$$

$$Q_{2l} \simeq \frac{m_l S_{22}}{\sqrt{2} h_2} \simeq \frac{m_l}{\sqrt{2} h_1} \tag{43}$$

where m_l denotes the lepton mass and we have used (25), (26) and (33). Equation (103) then gives

$$\Gamma(\tilde{\chi}_2^0 \xrightarrow{H_{1R}} \tilde{\chi}_1^0 l^+ l^-) \simeq 10^{-5}\lambda^2 \frac{M_1^3 m_l^2}{m_{H_{1R}}^4} I_2(\eta,\omega_2). \tag{44}$$

As before, the phase space integral I_2, given by (104), is of $O(10^{-1})$. The only leptonic final state with sizable couplings to the Higgses is the $\tau^+\tau^-$ pair. Taking for H_{1R} a mass of order 100 GeV, we get

$$\Gamma(\tilde{\chi}_2^0 \xrightarrow{H_{1R}} \tilde{\chi}_1^0 \tau^+ \tau^-) \sim 10^{-14}\lambda^2 \frac{M_1^3}{(1\text{GeV})^2}. \tag{45}$$

Even if one takes $M_1 = M_Z$, this is completely negligible compared to (40). The second pseudoscalar A^0 and the third scalar H_{2R} being much heavier than H_{1R} will give even smaller contributions.

To summarize, the dominant contribution to the $\tilde{\chi}_2^0 \to \tilde{\chi}_1^0 l^+ l^-$ transition is the slepton exchange, and we do not need to compute any interference term between diagrams. This remains valid for any value of η, although the partial width can become significantly smaller than (40) as the phase space is reduced for $|\eta| \to 1$.

Next, we turn to the neutrino production $\tilde{\chi}_2^0 \to \tilde{\chi}_1^0 \nu\bar{\nu}$. The Higgs exchange does not contribute. For the partial width via Z exchange, we get the same result as for charged leptons with an extra factor 2 from the $Z\nu\bar{\nu}$ vertex. As the sneutrino is a "left" type sfermion, the vertex factor required for the sneutrino exchange is slightly different:

$$\frac{1}{\sqrt{2}}(g_2 N_{11} - g_1 N_{12}) \simeq .17\lambda \left(\frac{M_Z}{M_1}\right)^2. \tag{46}$$

The partial width reads

$$\begin{aligned}\Gamma(\tilde{\chi}_2^0 \xrightarrow{\tilde{\nu}} \tilde{\chi}_1^0 \nu\bar{\nu}) &\simeq 10^{-6}\lambda^2 M_1 \left(\frac{M_Z}{m_{\tilde{\nu}}}\right)^4 I_{\tilde{\nu}}(\eta,\omega_{\tilde{\nu}})\\ &\gtrsim 10^{-8}\lambda^2 M_1.\end{aligned} \tag{47}$$

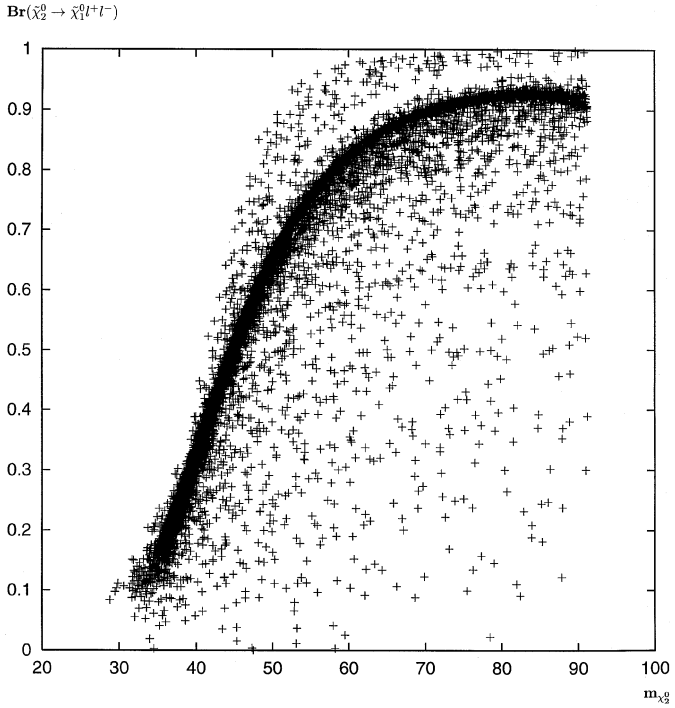

Fig. 4. Branching ratio of the charged lepton production $\tilde{\chi}_2^0 \to \tilde{\chi}_1^0 l^+ l^-$ versus the Bino mass $m_{\chi_2^0}$

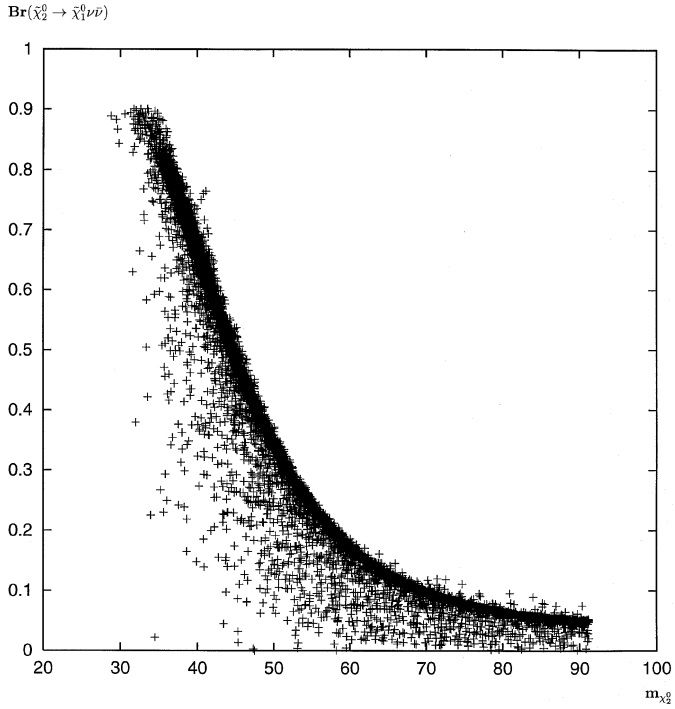

Fig. 5. Branching ratio of the neutrino production $\tilde{\chi}_2^0 \to \tilde{\chi}_1^0 \nu\bar{\nu}$ versus the Bino mass $m_{\chi_2^0}$

Although sneutrinos can be rather heavy (~ 150 GeV for $M_1 = M_Z$), this contribution always remains larger than the one from Z exchange. Thus, the virtual sneutrino exchange gives the main contribution to the $\tilde{\chi}_2^0 \to \tilde{\chi}_1^0 \nu\bar{\nu}$ channel and the computation of interference terms is not needed.

Finally we consider the decay into two jets $\tilde{\chi}_2^0 \to \tilde{\chi}_1^0 q\bar{q}$. The top is too heavy to be produced. The partial width via virtual Z exchange is of the same order as in the case of leptons (with an extra color factor $N_q = 3$ and slightly different $Zf\bar{f}$ couplings), whereas the squark exchange is strongly suppressed because squarks are always rather heavy. As for charged leptons, the virtual Higgs exchange plays no role. Hence, the virtual Z exchange is the only important contribution to the $\tilde{\chi}_2^0 \to \tilde{\chi}_1^0 q\bar{q}$ partial width, which therefore is always small compared to the partial width into two leptons via slepton exchange.

With the approximate expressions for the three body decays $\tilde{\chi}_2^0 \to \tilde{\chi}_1^0 l^+ l^-$, $\tilde{\chi}_2^0 \to \tilde{\chi}_1^0 \nu\bar{\nu}$ and $\tilde{\chi}_2^0 \to \tilde{\chi}_1^0 q\bar{q}$ at hand, we turn now to the "exact" numerical results. In Figs. 4-6 we present our numerical results for the branching ratios of the three body decays $\tilde{\chi}_2^0 \to \tilde{\chi}_1^0 l^+ l^-$, $\tilde{\chi}_2^0 \to \tilde{\chi}_1^0 \nu\bar{\nu}$ and $\tilde{\chi}_2^0 \to \tilde{\chi}_1^0 q\bar{q}$ ($q = u, d, c, s, b$) respectively, for $\sim 10^4$ points in the parameter space described in Sect. 2. Here we used exact expressions for the mixing factors, the phase space integrals and we included all contributions to a given final state.

From the previous discussion, the branching ratios do not depend on λ, since all the partial widths are proportional to λ^2, but essentially on the bino mass: For small values of $m_{\chi_2^0}$ (~ 30 GeV), sneutrinos are lighter than charged sleptons (~ 45 GeV and ~ 60 GeV respectively), therefore the main contribution to the total decay width is the neutrino production via virtual sneutrino exchange (Fig. 5). As the bino mass increases, the sneutrino mass gets larger than the charged slepton mass. The dominant process is then the charged lepton production via virtual slepton exchange (Fig. 4) (except for a small domain in the parameter space on which we shall come back in the next paragraph). As advertised earlier, the jet production (Fig. 6) is always small. In the domain of large bino masses, where sleptons are also relatively heavy, the quark production via virtual Z exchange can contribute up to $\sim 20\%$ to the total width. Genuinely we have

$$10^{-4} \lesssim \frac{\Gamma(\tilde{\chi}_2^0 \to \tilde{\chi}_1^0 q\bar{q})}{\Gamma(\tilde{\chi}_2^0 \to \tilde{\chi}_1^0 l^+ l^-)} \lesssim 10^{-1}. \tag{48}$$

Let us now study the two body decay into a real Higgs boson of Fig. 2, starting again with approximate analytic expressions. The lightest non-singlet scalar (which is mainly H_{1R}) is too heavy to be produced on shell. As already remarked in (41), one gets for the bino-singlino-singlet Higgs scalar vertex factor

$$Q_{112} \sim \lambda^2, \tag{49}$$

so that the partial width (110) [9] approximately reads

$$\Gamma(\tilde{\chi}_2^0 \to \tilde{\chi}_1^0 S_R) \sim \lambda^4 M_1. \tag{50}$$

For small values of λ, this is completely negligible compared to the three body decay rates. Yet, (50) involves no

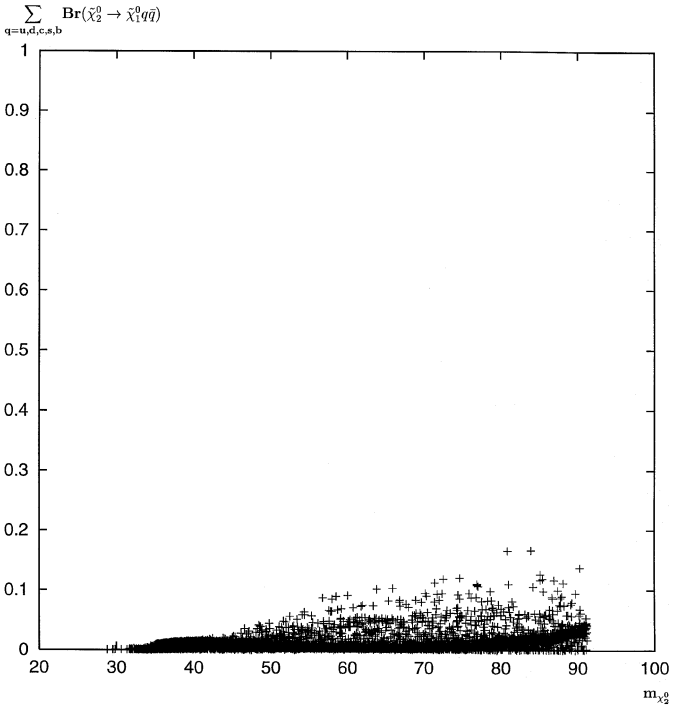

Fig. 6. Branching ratio of the jet production $\tilde{\chi}_2^0 \to \tilde{\chi}_1^0 q\bar{q}$ ($q = u, d, c, s, b$) versus the Bino mass $m_{\chi_2^0}$

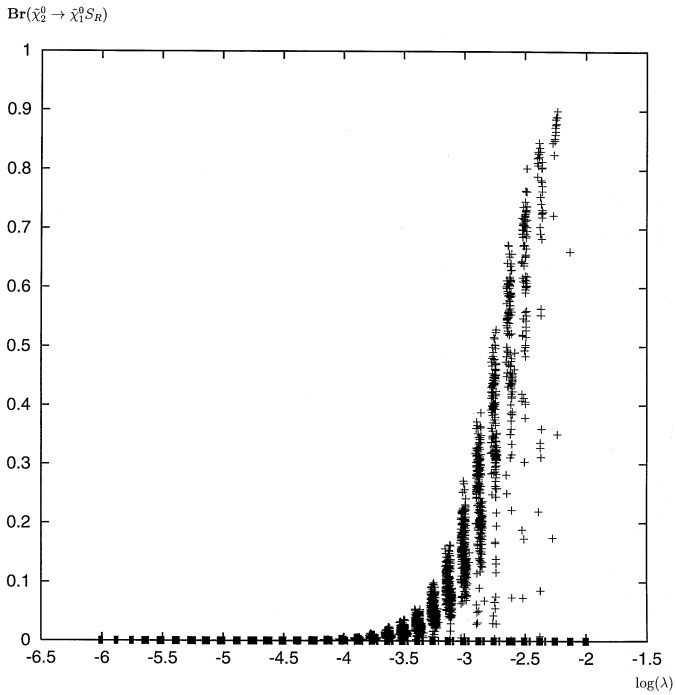

Fig. 7. Branching ratio of the real singlet Higgs scalar production $\tilde{\chi}_2^0 \to \tilde{\chi}_1^0 S_1$ versus $\log(\lambda)$

tiny numerical factor stemming from virtually exchanged particles. Hence, if λ is not too small, real Higgs singlet production can even dominate the total decay width. However, as emphasized in the previous section, the masses of $\tilde{S}$ and S_R are roughly proportional to $\lambda^{.5\pm.3} M_0$. Therefore, if λ is too large, the singlet Higgs scalar and the singlino become too heavy to be produced on shell in the bino decay and this channel is kinematically forbidden.

The numerical results are displayed in Fig. 7. They are in good agreement with our approximations and one finds that for a small window in λ, $\lambda \simeq 10^{-3}$, the branching ratio of this process can reach 90%. In the same window, we could have the two body decay with a real singlet Higgs pseudoscalar $\tilde{\chi}_2^0 \to \tilde{\chi}_1^0 S_I$. However, since the pseudoscalar singlet is always heavier than the scalar, this contribution remains small ($\lesssim$ 5%). If $\lambda \gtrsim 2.10^{-3}$, the emitted Higgs singlet is heavy enough to decay into $b\bar{b}$, which is then the main final state. For smaller values of λ, this channel is kinematically closed. Depending on the singlet mass, the $\tau^+\tau^-/c\bar{c}$ channels are then favored. Smaller singlet masses correspond to smaller values of λ, in which case the real Higgs singlet production is negligible.

Finally, we turn to the radiative decay $\tilde{\chi}_2^0 \to \tilde{\chi}_1^0 \gamma$. A complete calculation involves loops with fermions + sfermions and charginos + W, charged Higgs and Goldstone bosons (depending on the gauge choice) [10]. The corresponding contributions decrease with increasing masses of the particles inside the loops. In the following analytic approximation, we then only consider the dominant diagram, involving the lightest particles in the loops, namely the "right" type charged sleptons (Fig. 3). However, it is worth being stressed that we performed a complete numerical analysis, including all the loops mentioned above with the correct chargino and stop mass eigenstates [14]. The effective coupling (112) for three degenerate $\tilde{l}_R$ loops is given by

$$g_\gamma = \frac{3 e g_1^2 N_{12}}{16\pi^2} I_\gamma(\eta, \omega_{\tilde{l}_R}) \simeq 2.10^{-4} \lambda \left(\frac{M_Z}{M_1}\right)^2 I_\gamma(\eta, \omega_{\tilde{l}_R}) \qquad (51)$$

where I_γ, defined in (113), is of $O(10^{-1})$ if $|\eta| \not\to 1$. The partial width (111) then reads

$$\Gamma(\tilde{\chi}_2^0 \to \tilde{\chi}_1^0 \gamma) \sim 10^{-11} \lambda^2 \frac{M_Z^4}{M_1^3}. \qquad (52)$$

Even for small values of M_1, this is totally negligible compared to the three body decay rates. This is not surprising since it is a contribution of higher order in perturbation theory. Note that there is no "dynamical enhancement" mechanism for this channel in our model as it can appear in the MSSM under special assumptions [10,11]. However, there could be some "kinematical enhancement":

Up to now, we have assumed $|\eta| \ll 1$ (i.e. very light singlino) in all our analytic approximations. What happens for $|\eta| \to 1$? On the one hand, all the three body decay phase space integrals (98), (104) and (109) tend towards 0. As it has already been mentioned elsewhere [10, 11], one can check that they are all of order

$$I(\eta, \omega) \overset{|\eta|\to 1}{\sim} (1 - |\eta|)^5. \qquad (53)$$

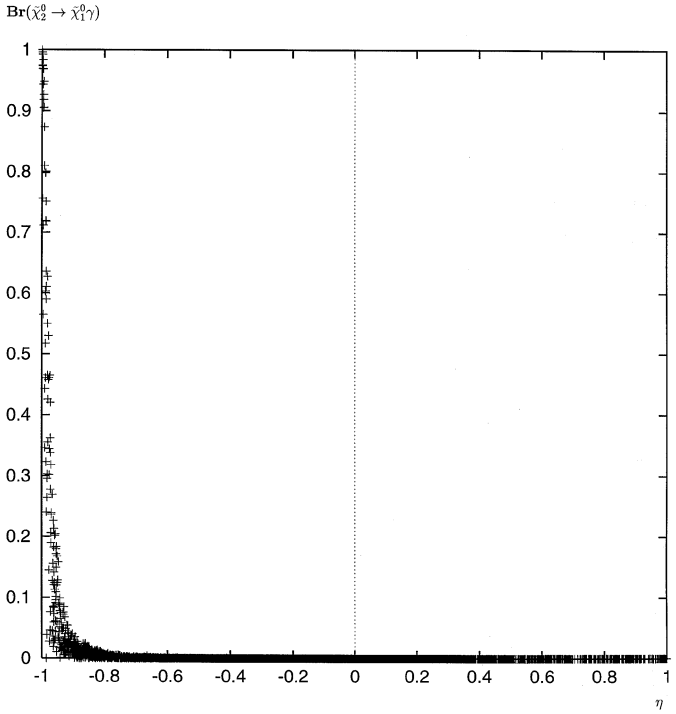

Fig. 8. Branching ratio of the radiative decay $\tilde{\chi}_2^0 \to \tilde{\chi}_1^0\gamma$ versus η

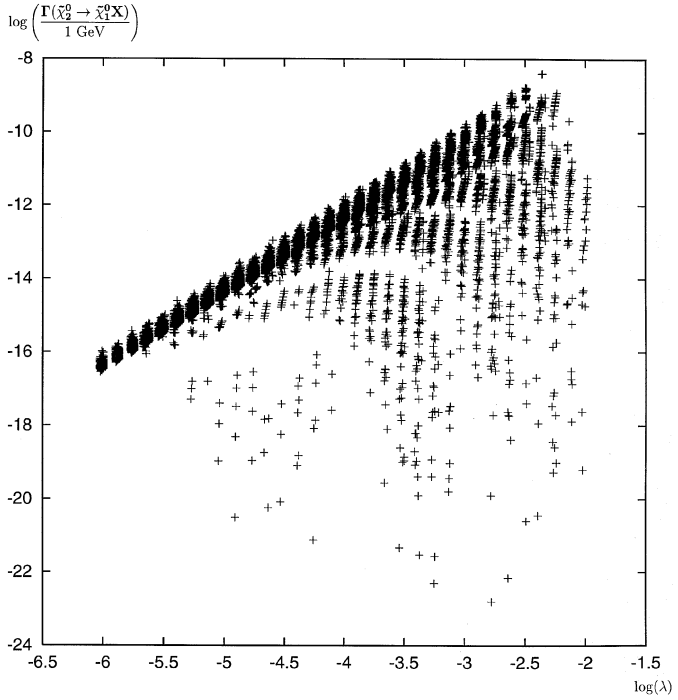

Fig. 9. Total decay width of the bino to singlino transition $\log(\Gamma(\tilde{\chi}_2^0 \to \tilde{\chi}_1^0 X))$ versus $\log(\lambda)$

Hence, all the $\tilde{\chi}_2^0 \to \tilde{\chi}_1^0 f\bar{f}$ channels are *equally* suppressed. Furthermore, since in this case the singlino mass is close to the bino mass, the two body decay with a real singlet Higgs boson is kinematically forbidden.

On the other hand, it is well known that the radiative decay $\tilde{\chi}_2^0 \to \tilde{\chi}_1^0\gamma$ is usually less suppressed for $|\eta| \to 1$. One can expand the loop integral (113) around $\eta = \pm 1$:

$$I_\gamma(\eta, \omega_{\tilde{l}_R}) \overset{\eta \to 1}{\sim} (1-\eta)^5 \overset{\eta \to -1}{\sim} (1+\eta)^3. \tag{54}$$

Therefore, the radiative decay gives the main contribution to the total decay width for $\eta \to -1$, but not for $\eta \to 1$. This phenomenon has not been observed before in the context of radiative neutralino decay. A similar effect exists for the neutrinoless double beta decay where the result depends on the relative sign of the Majorana neutrino masses [19]. This rough estimate correctly fits our numerical results for the branching ratio $Br(\tilde{\chi}_2^0 \to \tilde{\chi}_1^0\gamma)$, shown in Fig. 8. Actually, one finds that the main contributions to the radiative decay are the charged lepton/"right" slepton loops, the top/lighter stop loops and the lighter chargino/W loops [14]. Interferences between chargino and sfermion loops being destructive, this leads to even smaller branching ratios for the radiative decay, and this channel is kinematically enhanced only for a few points in the parameter space corresponding to $\eta \sim -1$.

To conclude, we give in Fig. 9 the total width of the bino to singlino transition, including all the contributions discussed above, as a function of λ. The λ^2 dependence is manifest for very small values of λ where the singlino is always very light. As λ increases, the singlino mass can take non negligible values, in which case the bino decay is kinematically suppressed. These cases correspond to the points in Fig. 9 below the "fat" diagonal line. From the total width it is straightforward to compute the bino lifetime:

$$\tau_{\tilde{\chi}_2^0} = \frac{\hbar}{\Gamma(\tilde{\chi}_2^0 \to \tilde{\chi}_1^0 X)} = \frac{6.58\,10^{-25}\mathrm{GeV.s}}{\Gamma(\tilde{\chi}_2^0 \to \tilde{\chi}_1^0 X)}. \tag{55}$$

For an energetic bino, the length of flight in the lab system is given by

$$l_{\tilde{\chi}_2^0} = \sqrt{\gamma^2 - 1}\, c\tau_{\tilde{\chi}_2^0} \simeq \frac{\hbar c}{\Gamma(\tilde{\chi}_2^0 \to \tilde{\chi}_1^0 X)} \simeq \frac{1.97\,10^{-16}\mathrm{GeV.m}}{\Gamma(\tilde{\chi}_2^0 \to \tilde{\chi}_1^0 X)} \tag{56}$$

One can then simply read off $l_{\tilde{\chi}_2^0}$ from Fig. 9. For $\Gamma(\tilde{\chi}_2^0 \to \tilde{\chi}_1^0 X) \lesssim 10^{-16}$ GeV (which corresponds to $\lambda \lesssim 5.10^{-6}$ or strong kinematical suppression), the bino escapes the detector, and the signature is the same as in the MSSM. In the other cases, we obtain the expected additional cascade, with a macroscopically displaced vertex ($l_{\tilde{\chi}_2^0} > 1$ mm) for $\Gamma(\tilde{\chi}_2^0 \to \tilde{\chi}_1^0 X) \lesssim 5.10^{-13}$ GeV.

5 Conclusions and outlook

The purpose of the present paper was the calculation of the NLSP partial and total decay widths in the (M+1)SSM, in the case where the LSP is a singlino and sparticle production is kinematically allowed at LEP2. Then, the NLSP

is essentially a bino and the bino to singlino transition appears at the end of all sparticle decay chains. (On the other hand, if the singlino is *not* the LSP, it will be nearly impossible to produce neither the singlino nor the Higgs singlet in collider experiments, since the singlet sector is always almost decoupled from the rest of the theory. The (M+1)SSM is then very difficult to disentangle from the MSSM.)

We worked in the context of the constrained (M+1)SSM, with universal boundary conditions for the soft terms at the GUT scale. The essential features of this scenario have been discussed, using analytic approximations, in Sect. 3. We have seen that, while the singlino LSP scenario is not a necessary consequence of the model, it corresponds to a natural "gaugino dominated" scenario, gaugino masses being the largest soft terms. Furthermore, the singlino is automatically the LSP for very small Yukawa couplings λ and κ.

The gross features of the bino decay widths are easy to understand using analytic approximations. In Sect. 4 we have presented and discussed such approximate analytic expressions for the partial decay widths, which are in good agreement with the results obtained numerically (without the corresponding approximations). The numeric results have been presented in the form of the Figs. 3-9. (The corresponding detailed formulae are given in the appendices.)

Let us summarize the behavior of the total decay width $\Gamma(\tilde{\chi}_2^0 \to \tilde{\chi}_1^0 X)$. In principle, the bino partial and total decay widths can vary over many orders of magnitude, depending on the Yukawa coupling λ, the bino mass $m_{\chi_2^0} \sim M_1$ and the singlino to bino mass ratio η (with $\eta \to 0$ for $\lambda \to 0$). Generally one has

$$\Gamma(\tilde{\chi}_2^0 \to \tilde{\chi}_1^0 X) \lesssim 10^{-6} \lambda^2 M_1. \tag{57}$$

For $|\eta| \ll 1$, the inequality (57) can roughly be replaced by an equality. For $|\eta| \to 1$, however, $\Gamma(\tilde{\chi}_2^0 \to \tilde{\chi}_1^0 X)$ can be considerably smaller than the right hand side of (57) because of kinematical suppression. The allowed range of the total decay width as a function of λ is displayed in Fig. 9, and the corresponding bino lifetime can lead to macroscopically displaced vertices. For very small values of $\Gamma(\tilde{\chi}_2^0 \to \tilde{\chi}_1^0 X)$, the bino may even decay outside the detector (in which case it imitates the true LSP of the MSSM). However, this requires tiny Yukawa couplings ($\lambda \lesssim 5.10^{-6}$) or strong kinematical suppression. Such scenarios could be probed by the same kind of apparatus as the slow neutralino to gravitino transition in the context of Gauge Mediated Supersymmetry Breaking models [15].

For a given value of $\Gamma(\tilde{\chi}_2^0 \to \tilde{\chi}_1^0 X)$, the branching ratios of the bino still vary essentially with the bino and singlino masses. In most of the parameter space, the three body decay (Fig. 1) dominates, and the relevant final states are $\nu\bar{\nu}$, l^+l^- or $q\bar{q}$ ($q = u, d, c, s, b$) and missing energy. For small values of the bino mass ($\sim$ 30 GeV), the $\nu\bar{\nu}$ channel dominates (Fig. 5). Hence, the bino decays invisibly and its signature is just missing energy as for the true LSP of the MSSM. However, this channel never exceeds 90%, the remaining 10% corresponding to the visible l^+l^- channel (Fig. 4). For larger values of the bino mass (up to M_Z), on the other hand, the invisible final state $\nu\bar{\nu}$ becomes less important and the charged lepton channel contributes up to 100%. The partial width into $q\bar{q}$ is always small compared to the partial width into l^+l^-, and we expect at most one jet event for ten charged lepton events. The characteristic signature for sparticle production would then be lepton events with high multiplicity (at least four, in $e^+e^- \to \tilde{\chi}_2^0\tilde{\chi}_2^0$) plus missing energy, eventually with displaced vertices.

However, in the window $10^{-3} \lesssim \lambda \lesssim 10^{-2}$, the two body decay $\tilde{\chi}_2^0 \to \tilde{\chi}_1^0 S_1$ dominates, if kinematically allowed (Fig. 7). S_1 is then essentially the Higgs singlet with a mass varying between 3 and 35 GeV. If its mass is larger than $\sim$ 10 GeV, S_1 decays into $b\bar{b}$ (with a branching ratio of $\sim$ 90%); otherwise, $\tau^+\tau^-/c\bar{c}$ are favored. (For such values of λ, the bino and the real Higgs singlet will have short lifetimes.) The relevant final state would be two b-jets (or eventually $\tau^+\tau^-/c$-jets) with an invariant mass peaked below 35 GeV. Such processes are totally exluded in the MSSM and would be a strong sign for the (M+1)SSM.

Finally, in the degenerate case $\eta \sim -1$, all the previous tree level channels are kinematically suppressed, and the radiative decay $\tilde{\chi}_2^0 \to \tilde{\chi}_1^0\gamma$ dominates (Fig. 8). In such a scenario, the bino would be very long lived ($l_{\tilde{\chi}_2^0} \gtrsim 1$ m). (This corresponds, however, to a tiny fraction of the parameter space.) In contrast to the MSSM [11], a dominance of the radiative decay is compatible with universal soft terms, and the (rather disfavored) condition $\tan\beta \sim 1$ is not required in the (M+1)SSM.

Herewith we have summarized our results, which have been obtained for $m_{\chi_2^0} < M_Z$, the range accessible at LEP2. Let us, at the end, comment on the case of a bino which is heavier than the Z. One should consider two different regimes:

In the intermediate range $M_Z < m_{\chi_2^0} \lesssim$ 130 GeV, the main decay mode becomes $\tilde{\chi}_2^0 \to \tilde{\chi}_1^0 Z$, with $\tilde{\chi}_1^0$ and Z on shell. The total decay width is again proportional to λ^2, though larger than in the case of the three body decay (since no virtual particle needs to be exchanged). Hence, the bino would not be too long lived in this case, except for extremely small values of λ. The characteristic signature for this additionnal cascade is missing energy plus the typical Z decay products.

For a very heavy bino, $m_{\chi_2^0} \gtrsim$ 130 GeV, one has $m_{\chi_2^0} > m_{\tilde{l}_R}$ as already noticed in (29). The "right" charged sleptons are hence light enough to be produced on shell, and the main channel is $\tilde{\chi}_2^0 \to l\tilde{l}_R$. Since one needs at least $m_{\chi_2^0} \gtrsim$ 250 GeV in order to have $m_{\chi_2^0} - m_{\tilde{l}_R} \gtrsim$ 10 GeV, the emitted lepton is very soft, hence difficult to detect. Yet, in this case, the true NLSP is the charged slepton and the process of interest is $\tilde{l}_R \to l^\pm\tilde{\chi}_1^0$, appearing at the end of all sparticle decay chains. Then one obtains a charged slepton (eventually long lived, depending on λ) decaying into an energetic lepton plus missing energy (the singlino). This case corresponds, however, to a very heavy sparticle spectrum, disfavored by solutions to the hierarchy problem.

Acknowledgements. It is a pleasure to thank L. Duflot and C.A. Savoy for valuable discussions.

Appendix

A Neutralino sector

The mass terms for the neutralinos are given by the following part of the lagrangian:

$$\begin{aligned}\mathcal{L} = &\frac{ig_1}{\sqrt{2}}(-h_1\lambda_1\psi_1 + h_2\lambda_1\psi_2) + \frac{ig_2}{\sqrt{2}}(h_1\lambda_2^3\psi_1 - h_2\lambda_2^3\psi_2)\\ &+\lambda s\psi_1\psi_2 + \lambda h_1\psi_2\psi_s + \lambda h_2\psi_1\psi_s - \kappa s\psi_s\psi_s\\ &+\frac{1}{2}M_1\lambda_1\lambda_1 + \frac{1}{2}M_2\lambda_2^3\lambda_2^3 + \text{h.c.}\end{aligned} \tag{58}$$

where the two component spinors λ_1, λ_2^3, ψ_1, ψ_2 and ψ_s are the supersymmetric partners of the B, W^3, H_1^0, H_2^0 and S bosons respectively. We introduce the 5 component neutralino vector [16]:

$$(\psi^0)^T = (-i\lambda_2^3, -i\lambda_1, \psi_1, \psi_2, \psi_s). \tag{59}$$

Then the mass terms read

$$\mathcal{L} = -\frac{1}{2}(\psi^0)^T M^0 (\psi^0) + \text{h.c.} \tag{60}$$

where the (symmetric) neutralino mass matrix M^0 is given by

$$M^0 = \begin{pmatrix} M_2 & 0 & \frac{-g_2h_1}{\sqrt{2}} & \frac{g_2h_2}{\sqrt{2}} & 0 \\ & M_1 & \frac{g_1h_1}{\sqrt{2}} & \frac{-g_1h_2}{\sqrt{2}} & 0 \\ & & 0 & -\mu & -\lambda h_2 \\ & & & 0 & -\lambda h_1 \\ & & & & 2\kappa s \end{pmatrix}. \tag{61}$$

The physical mass eigenstates are obtained by diagonalizing $\mathcal{M}^0$ with a unitary matrix N:

$$m_{\chi_i^0}\delta_{ij} = N_{im}N_{jn}M^0_{mn} \tag{62}$$

$m_{\chi_i^0}$ being the mass eigenvalues in increasing order of the neutralino states:

$$\chi_i^0 = N_{ij}\psi_j^0 \quad i = 1, \ldots, 5. \tag{63}$$

We take N real and orthogonal. Then some of the mass eigenvalues may be negative. Finally, one obtains the proper 4 component neutralino eigenstates by defining the Majorana spinors:

$$\tilde{\chi}_i^0 = \begin{pmatrix} \chi_i^0 \\ \bar{\chi}_i^0 \end{pmatrix} \quad i = 1, \ldots, 5. \tag{64}$$

B Higgs sector

We give here the potential, the minimization equations and the mass matrix for the neutral scalar Higgs without radiative corrections. The purpose of this appendix is only to set up our conventions and to provide some guidelines in order to make our analytic approximations easier to understand. A more complete analysis of this sector can be found in [3].

The scalar potential for the neutral Higgs fields is given by

$$\begin{aligned}V = &\lambda^2(|H_1^0|^2|S|^2 + |H_2^0|^2|S|^2 + |H_1^0|^2|H_2^0|^2) + \kappa^2|S^2|^2\\ &-\lambda\kappa(H_1^0H_2^0S^{*2} + \text{h.c.}) + \frac{g^2}{4}(|H_1^0|^2 - |H_2^0|^2)^2\\ &+m_1^2|H_1^0|^2 + m_2^2|H_2^0|^2 + m_S^2|S|^2\\ &-\lambda A_\lambda(H_1^0H_2^0S + \text{h.c.}) + \frac{\kappa A_\kappa}{3}(S^3 + \text{h.c.})\end{aligned} \tag{65}$$

where $g^2 = \frac{1}{2}(g_1^2 + g_2^2)$. We split the Higgs fields into real and imaginary parts:

$$\begin{aligned}&H_1^0 = h_1 + \frac{H_{1\,R}^0 + iH_{1\,I}^0}{\sqrt{2}}, \quad H_2^0 = h_2 + \frac{H_{2\,R}^0 + iH_{2\,I}^0}{\sqrt{2}},\\ &S = s + \frac{S_R + iS_I}{\sqrt{2}}.\end{aligned} \tag{66}$$

The conditions for extrema of (65) are

$$\begin{aligned}h_1(\lambda^2(h_2^2 + s^2) + \frac{g^2}{2}(h_1^2 - h_2^2) + m_1^2)&\\ -\lambda h_2 s(A_\lambda + \kappa s) = 0,& \quad (67)\\ h_2(\lambda^2(h_1^2 + s^2) - \frac{g^2}{2}(h_1^2 - h_2^2) + m_2^2)&\\ -\lambda h_1 s(A_\lambda + \kappa s) = 0,& \quad (68)\\ s(\lambda^2(h_1^2 + h_2^2) + 2\kappa^2 s^2 - 2\lambda\kappa h_1h_2 + m_S^2)&\\ -\lambda A_\lambda h_1h_2 + \kappa A_\kappa s^2 = 0.& \quad (69)\end{aligned}$$

After the elimination of m_1^2, m_2^2 and m_S^2 using (67-69), the elements of the 3x3 symmetric mass matrix for the CP-even scalars in the basis $(H_{1\,R}^0, H_{2\,R}^0, S_R)$ are

$$M_{S,11}^2 = g^2h_1^2 + \lambda s\frac{h_2}{h_1}(A_\lambda + \kappa s), \tag{70}$$

$$M_{S,22}^2 = g^2h_2^2 + \lambda s\frac{h_1}{h_2}(A_\lambda + \kappa s), \tag{71}$$

$$M_{S,33}^2 = \lambda A_\lambda\frac{h_1h_2}{s} + \kappa s(A_\kappa + 4\kappa s), \tag{72}$$

$$M_{S,12}^2 = (2\lambda^2 - g^2)h_1h_2 - \lambda s(A_\lambda + \kappa s), \tag{73}$$

$$M_{S,13}^2 = 2\lambda^2h_1s + \lambda h_2(A_\lambda + 2\kappa s), \tag{74}$$

$$M_{S,23}^2 = 2\lambda^2h_2s + \lambda h_1(A_\lambda + 2\kappa s). \tag{75}$$

Likewise, the elements of the 2x2 mass matrix for the CP-odd pseudoscalars in the basis (A^0, S_I) where the would-be Goldstone boson has been projected out, read

$$M_{P,11}^2 = \lambda s(A_\lambda + \kappa s)\frac{h_1^2 + h_2^2}{h_1h_2}, \tag{76}$$

$$M^2_{P,22} = \lambda(A_\lambda + 4\kappa s)\frac{h_1 h_2}{s} - 3\kappa A_\kappa s, \quad (77)$$

$$M^2_{P,12} = \lambda(A_\lambda - 2\kappa s)\sqrt{h_1^2 + h_2^2}. \quad (78)$$

The mass eigenstates of the scalars are denoted by $S_{a=1,2,3}(m_{S_1} \leq m_{S_2} \leq m_{S_3})$ and those of the pseudoscalars by $P_{\alpha=1,2}(m_{P_1} \leq m_{P_2})$.

C Approximate results of the integrated RGEs

In this appendix we display some simple analytic results of the integrated RGEs in the approximation where the dependence on all Yukawa couplings but the one of the top quark, h_t, are neglected. Such solutions have been first discussed in the MSSM framework in [17]. The Renormalization Group Equations for the (M+1)SSM can be found in [2]. We assume universality for the soft terms at the GUT scale and no flavor mixing. For a more complete and general set of solutions, cf [18].

First, let us define the parameter ρ by

$$\rho = \frac{h_t^2}{h_{crit}^2} \quad (79)$$

where h_{crit} is the infra-red fixed point solution for h_t, $h_{crit} \simeq 1.13$. We find from our numerical results with a singlino LSP: $.7 \lesssim \rho \lesssim .8$.

The Yukawa couplings λ and κ are only slightly renormalized:

$$\lambda \simeq \lambda_0 \quad , \quad \kappa \simeq \kappa_0. \quad (80)$$

The results for the soft trilinear terms read

$$A_\lambda = A_0\left(1 - \frac{\rho}{2}\right) + (1.11\rho - .59)M_0, \quad (81)$$

$$A_\kappa = A_0. \quad (82)$$

Soft scalar masses are as follows

$$m_S^2 = m_0^2, \quad (83)$$

$$m_1^2 = \left(1 - \frac{3}{2}\rho\right)m_0^2 - \frac{\rho(1-\rho)}{2}(A_0 - 2.22M_0)^2 + (.52 - 3.71\rho)M_0^2, \quad (84)$$

$$m_2^2 = m_0^2 + .52M_0^2, \quad (85)$$

$$m_L^2 = m_0^2 + .52M_0^2, \quad (86)$$

$$m_E^2 = m_0^2 + .15M_0^2. \quad (87)$$

Finally, we have the usual gaugino mass relations

$$M_2 = .82M_0, \quad M_1 = \frac{5}{3}\frac{g_1}{g_2}M_2 \simeq \frac{1}{2}M_2 = .41M_0. \quad (88)$$

D Decay widths

We first repeat some general features of the three body decay of $\tilde\chi_2^0$ with mass $m_{\chi_2^0}$ and momentum p_2 into $\tilde\chi_1^0$ with mass $m_{\chi_1^0}$ and momentum p_1 and two massless fermions f and $\bar f$ with momenta k and k' respectively.

Using the Mandelstam variables

$$s = (p_2 - p_1)^2, \quad t = (p_2 - k)^2, \quad u = (p_1 - k)^2, \quad (89)$$

the differential decay width can be written as

$$d\Gamma = \frac{N_f}{512\pi^3 m^3_{\chi_2^0}} \sum_{spins} |\mathcal{M}|^2 du dt \quad (90)$$

where $\mathcal{M}$ is the invariant amplitude for the processes under consideration and N_f is the color factor of the fermions. The different diagrams are shown in Fig. 1. As seen in the main part of the paper, we only need the integrated width for each process separately, without interference term (except in the case of sfermion exchange, see below). The integration limits are

$$\begin{cases} 0 \leq s \leq (|m_{\chi_2^0}| - |m_{\chi_1^0}|)^2 \\ t_{min,max} = \frac{1}{2}\left(m^2_{\chi_2^0} - m^2_{\chi_1^0} - s \pm \sqrt{\lambda(m^2_{\chi_2^0}, m^2_{\chi_1^0}, s)}\right) \\ u + t + s = m^2_{\chi_2^0} + m^2_{\chi_1^0} \end{cases} \quad (91)$$

λ being the usual triangle function:

$$\lambda(a,b,c) = a^2 + b^2 + c^2 - 2ab - 2ac - 2bc. \quad (92)$$

To begin with, let us consider the Z exchange. We use the following notations:

– The parameters in the Z-fermions coupling are

$$L_f = T_{3f} - Q_f \sin^2\theta_W, \quad R_f = -Q_f \sin^2\theta_W \quad (93)$$

where T_{3f} and Q_f are the isospin and the charge of the fermion respectively.

– The Z propagator is given by

$$D_Z(x) = (x - M_Z^2 + iM_Z\Gamma_Z)^{-1}. \quad (94)$$

– The parameter in the $Z\tilde\chi_1^0\tilde\chi_2^0$ coupling is

$$O_{12} = N_{13}N_{23} - N_{14}N_{24} \quad (95)$$

where N_{ij} denote the mixing components of the neutralinos as given by (63).

The invariant amplitude of the process is [9]

$$\sum_{spins} |\mathcal{M}_Z|^2 = 4g^4(L_f^2 + R_f^2)O_{12}^2 |D_Z(s)|^2 \times \times \left((m^2_{\chi_2^0} - t)(t - m^2_{\chi_1^0}) + t \leftrightarrow u + 2m_{\chi_2^0}m_{\chi_1^0}s\right). \quad (96)$$

Hence, the partial width reads

$$\Gamma(\tilde\chi_2^0 \xrightarrow{Z} \tilde\chi_1^0 f\bar f) = \frac{N_f g^4(L_f^2 + R_f^2)O_{12}^2}{16\pi^3}\frac{m^5_{\chi_2^0}}{M_Z^4} I_Z(\eta, \omega_Z). \quad (97)$$

I_Z is a phase space integral depending on η defined in (16) and $\omega_Z = m_{\chi_2^0}/M_Z$:

$$I_Z(\eta,\omega_Z) = \frac{1}{3}\int_{\frac{1-\eta^2}{2}}^{1-|\eta|} dz \frac{\Delta(4z-1-2\eta+3\eta^2)(1+\eta-z)}{(\omega_Z^2(2z+\eta^2-1)-1)^2} \quad (98)$$

with $\Delta = \sqrt{(1-z)^2-\eta^2}$.

Next we turn to the Higgs exchange. We only display formulae for a CP-even Higgs S_a. The $S_a\tilde{\chi}_1^0\tilde{\chi}_2^0$ coupling reads

$$\begin{aligned} Q_{a12} = \frac{\lambda}{\sqrt{2}}&(S_{a1}(N_{15}N_{24}+N_{14}N_{25}) \\ &+S_{a2}(N_{15}N_{23}+N_{13}N_{25}) \\ &+S_{a3}(N_{13}N_{24}+N_{14}N_{23})) - \sqrt{2}\kappa S_{a3}N_{15}N_{25} \\ &+\frac{1}{2}(g_2N_{11}-g_1N_{12})(N_{23}S_{a1}-N_{24}S_{a2}) \\ &+\frac{1}{2}(g_2N_{21}-g_1N_{22})(N_{13}S_{a1}-N_{14}S_{a2}) \end{aligned} \quad (99)$$

where S_{ai} denote the mixing components of S_a in the basis (66). The Higgs-fermion coupling is

$$Q_{af} = \frac{m_f S_{a1}}{\sqrt{2}\,h_1} \quad \text{for an up-type quark,} \quad (100)$$

$$Q_{af} = \frac{m_f S_{a2}}{\sqrt{2}\,h_2} \quad \text{for a down-type quark or a charged lepton} \quad (101)$$

where m_f is the fermion mass. With the Higgs propagator D_a, the invariant amplitude reads

$$\sum_{spins}|\mathcal{M}_a|^2 = 4Q_{a12}^2Q_{af}^2|D_a(s)|^2(m_{\chi_2^0}^2+m_{\chi_1^0}^2+m_{\chi_2^0}m_{\chi_1^0}-s)s, \quad (102)$$

leading to the following partial width:

$$\Gamma(\tilde{\chi}_2^0 \xrightarrow{S_a} \tilde{\chi}_1^0 f\bar{f}) = \frac{N_f Q_{a12}^2 Q_{af}^2}{16\pi^3}\frac{m_{\chi_2^0}^5}{m_{S_a}^4} I_a(\eta,\omega_a) \quad (103)$$

where the phase space integral I_a depends on η and $\omega_a = m_{S_a}/m_{\chi_2^0}$:

$$I_a(\eta,\omega_a) = \int_{\frac{1-\eta^2}{2}}^{1-|\eta|} dz \frac{\Delta\omega_a^4(2z-1+\eta^2)(1+\eta-z)}{(2z+\eta^2-\omega_a^2-1)^2}. \quad (104)$$

Finally, we consider the sfermion exchange. Neglecting the fermion Yukawa coupling, the $\tilde{\chi}_i^0 f\tilde{f}_R$ vertex is

$$f_i = g_1\sqrt{2}\,Q_f N_{i2}, \quad (105)$$

and for the $\tilde{\chi}_i^0 f\tilde{f}_L$ vertex one gets

$$f_i = \sqrt{2}\,(g_2T_{3f}N_{i1} - g_1(T_{3f}-Q_f)N_{i2}). \quad (106)$$

With the sfermion propagator $D_{\tilde{f}}$, the invariant amplitude reads [9]

$$\begin{aligned} \sum_{spins}|\mathcal{M}_{\tilde{f}}|^2 = f_1^2f_2^2\Big((m_{\chi_2^0}^2-t)(t-m_{\chi_1^0}^2)|D_{\tilde{f}}(t)|^2 + t\leftrightarrow u \\ +2m_{\chi_2^0}m_{\chi_1^0}sD_{\tilde{f}}(t)D_{\tilde{f}}(u)\Big). \end{aligned} \quad (107)$$

The last term is an interference term. The partial width is then given by

$$\Gamma(\tilde{\chi}_2^0 \xrightarrow{\tilde{f}} \tilde{\chi}_1^0 f\bar{f}) = \frac{N_f f_1^2 f_2^2}{64\pi^3}\frac{m_{\chi_2^0}^5}{m_{\tilde{f}}^4} I_{\tilde{f}}(\eta,\omega_{\tilde{f}}). \quad (108)$$

$I_{\tilde{f}}(\eta,\omega_{\tilde{f}})$ is the phase space integral, depending on η and $\omega_{\tilde{f}} = m_{\chi_2^0}/m_{\tilde{f}}$:

$$\begin{aligned} I_{\tilde{f}}(\eta,\omega_{\tilde{f}}) = &\frac{1}{4}\int_{\eta^2}^1 dx \frac{(1-x)^2(x-\eta^2)^2}{(\omega_{\tilde{f}}^2x-1)^2x} \\ &+\eta\int_{\frac{1-\eta^2}{2}}^{1-|\eta|} dz \int_{\frac{z-\Delta}{2}}^{\frac{z+\Delta}{2}} dx \\ &\times\frac{2z+\eta^2-1}{(\omega_{\tilde{f}}^2(1-2x)-1)(\omega_{\tilde{f}}^2(1-2z+2x)-1)}. \end{aligned} \quad (109)$$

Now, we turn to the two body decay. The decay rate for the on-shell scalar Higgs production of Fig. 2 reads

$$\Gamma(\tilde{\chi}_2^0 \to \tilde{\chi}_1^0 S_a) = \frac{Q_{a12}^2 m_{\chi_2^0}}{16\pi}\sqrt{\lambda(1,\eta^2,\omega_a^2)}\,(1+2\eta+\eta^2-\omega_a^2). \quad (110)$$

Finally, let us consider the radiative decay $\tilde{\chi}_2^0 \to \tilde{\chi}_1^0\gamma$. The analytic approximation used in the main part of the paper includes only charged lepton/"right" slepton loops (for details, see [10,14]). The different contributions are shown in Fig. 3. The decay width reads

$$\Gamma(\tilde{\chi}_2^0 \to \tilde{\chi}_1^0\gamma) = \frac{g_{\chi\chi\gamma}^2(m_{\chi_2^0}^2-m_{\chi_1^0}^2)^3}{8\pi m_{\chi_2^0}^5}. \quad (111)$$

$g_{\chi\chi\gamma}$ is an effective coupling:

$$g_{\chi\chi\gamma} = \frac{e}{16\pi^2}\sum_f N_f Q_f f_1 f_2 I_\gamma(\eta,\omega_{\tilde{f}}) \quad (112)$$

where $f_{1,2}$ are given in (105) and

$$I_\gamma(\eta,\omega_{\tilde{f}}) = \frac{1}{1-\eta^2}\int_0^1 dx\left(1+\eta+\frac{1-\eta\omega_{\tilde{f}}^2x}{(1-\eta)\omega_{\tilde{f}}^2x}\log\left(\frac{1-\omega_{\tilde{f}}^2x}{1-\eta^2\omega_{\tilde{f}}^2x}\right)\right). \quad (113)$$

References

1. P. Fayet, Nucl. Phys. **B 90** (1975) 104;
   H.P. Nilles, M. Srednicki, D. Wyler, Phys. Lett. **B 120** (1983) 346;
   J. Ellis, J.F. Gunion, H.E. Haber, L. Roszkowski, F. Zwirner, Phys. Rev. **D 39** (1989) 844;
   L. Durand and J.L. Lopez, Phys. Lett. **B 217** (1989) 463;
   M. Drees, Int. J. Mod. Phys. **A 4** (1989) 3635
2. J.P. Derendinger, C.A. Savoy, Nucl. Phys. **B 237** (1984) 307
3. U. Ellwanger, Phys. Lett. **B 303** (1993) 271;
   U. Ellwanger, M. Rausch de Traubenberg, C.A. Savoy, Z. Phys. **C 67** (1995) 665;
   T. Elliott, S.F. King, P.L. White, Phys. Rev. **D 49** (1994) 2435
4. U. Ellwanger, M. Rausch de Traubenberg, C.A. Savoy, Phys. Lett. **B 315** (1993) 331;
   S.F. King, P.L. White, Phys. Rev. **D 52** (1995) 4183
5. U. Ellwanger, M. Rausch de Traubenberg, C.A. Savoy, Nucl. Phys. **B 492** (1997) 21
6. S.A. Abel, S. Sarkar, P.L. White, Nucl. Phys. **B 454** (1995) 663;
   S.A. Abel, Nucl. Phys. **B 480** (1996) 55-72; hep-ph 9603301
7. F. Franke, H. Fraas, Z. Phys. **C 72** (1996) 309
8. A. Stephan, hep-ph 9709262; hep-ph/9704232 (to appear in Phys. Lett. **B**)
9. A. Bartl, H. Fraas, W. Majerotto, Nucl. Phys. **B 278** (1986) 1
10. H.E. Haber, D. Wyler, Nucl. Phys. **B 323** (1989) 267
11. S. Ambrosanio, B. Mele, Phys. Rev. **D 55** (1997) 1399; **D 56** (1997) 3157
12. M. Gallinaro, CDF Collab., FERMILAB-CONF-97/004-E
13. J.F. Grivaz, hep-ph/9709505
14. C. Hugonie, unpublished
15. K. Maki, S. Orito, hep-ph/9706382
16. H.E. Haber, G.L. Kane, Phys. Rep. **117** (1985) 75
17. L.E. Ibañez, C. Lopez, Nucl. Phys. **B 233** (1984) 511;
    C. Kounnas, A.B. Lahanas, D.V. Nanopoulos, M. Quirós, Nucl. Phys. **B 236** (1984) 438;
    A. Bouquet, J. Kaplan, C.A. Savoy, Nucl. Phys. **B 262** (1985) 299
18. P. Brax, C.A. Savoy, Nucl. Phys. **B 447** (1995) 227
19. L. Wolfenstein, Phys. Lett. **B 107** (1981) 77